INTERNATIONAL JOURNAL OF AGRICULTURE & BIOLOGY
ISSN Print: 1560–8530; ISSN Online: 1814–9596
20F–102/202x/00–0–000–000
DOI: 10.17957/IJAB/15.1569
http://www.fspublishers.org

Full Length Article

Substrate Recognition Site 5 of CYP51 Protein Contributes to Azole Binding in Rice Blast Fungus *Maganporthe oryzae*

Weifang Liao[1*], Tingting Liu[2], Weijie Liao[3] and Jiaoyan Yang[2]
[1]*School of biology and pharmaceutical engineering, Wuhan Polytechnic University, Wuhan, 430023, P.R. China*
[2]*School of Life Sciences, Central China Normal University, Wuhan, 430079, P.R. China*
[3]*School of Life Sciences, Tsinghua University, Beijing, 100084, P.R. China*
[*]For correspondence: leesalwf89@126.com
Received 01 January 2020; Accepted 13 June 2020; Published ___________________

Abstract

Azole compounds used in agriculture to combat *Maganporthe oryzae,* the causal agent of rice blast disease, represent effective inhibitors of the sterol 14*α*-demethylase (CYP51) which is related to the formation of ergosterol. Since most of them exhibit a similar mode of action, resistance has become even more severe. Detailed research on the structural characteristics of CYP51 may help to develop more effective drugs. In this study, the azole binding potency of key conserved residues of two substrate recognition sites of CYP51 protein from *M. oryzae* (MoCYP51B) was investigated via site directed mutagenesis followed by spectral analysis. According to results of binding spectra in the presence of diniconazole, the K_d values of MoCYP51B with mutations I367W and V374Y was significantly ($P < 0.05$) increased in comparison to wild-type controls, indicating that the residues I367 and V374 of the MoCYP51B substrate recognition site 5 had critical contribution to azole binding. This study may provide useful insights into the studies and designs of novel antifungal agents for *M. oryzae.* © 2020 Friends Science Publishers

Keywords: Azoles; Binding spectrum; CYP51; *Magnaporthe oryzae*; Site-directed mutagenesis

Introduction

Magnaporthe oryzae (Hebert) ME Barr, an ascomycete fungus, causes blast disease in rice (Yang *et al.* 2009; Yan *et al.* 2013). Every year, this disease wreaked havoc incurring millions of dollars' economic losses (Chen *et al.* 2019). The continuous decrease in cultivable land and limited water resource further aggravate the problem (Talbot 2003). Until now, the fungal pathogen was controlled by using fungicides (Liu *et al.* 2012; Lopez and Cumagun 2019; Jeon *et al.* 2020). Since 1970s, various azole fungicides like propiconazole, diniconazole, triadimefon, triadimenol and tebuconazole have been widely used to prevent the attack of fungal pathogens. Since most of these modern fungicides exhibit a similar mode of action, resistant strains have re-surfaced, resulting in infected crops and the situation were exacerbated (Parker *et al.* 2011; Chowdhary *et al.* 2012; Price *et al.* 2015).

Most of the azole fungicides are the inhibitors of the biosynthesis of ergosterol, the predominant sterol component of the fungal cell membrane (Yang *et al.* 2009). The process is initiated by the binding of azoles with the CYP51 protein (Parker *et al.* 2011). Conserved residues of CYP51s are mostly clustered into 6 substrate recognition sites (SRSs) and the heme binding region (Lepesheva and Waterman 2007). Based on the crystal structure of CYP51 from *Aspergillus fumigatu*s, SRS1 (helix B'' and B'C loop), SRS2 (helix F''), helix C, SRS4 (the N-terminal portion of helix I), SRS5 (K helix-β1–4 loop) and SRS6 (β4 hairpin) form the active cavity related to substrate recognition and interaction (Hargrove *et al.* 2015). Some relationships of structure and function have been thoroughly studied on SRS regions, elucidated the importance of specific residues (Lamb *et al*. 1998; Hargrove *et al.* 2011). Mutation of these specific residues lowered the binding affinity of azoles without affecting expression of the protein. Unlike many other classes of fungicide where a single amino acid substitution in the target protein would lead to drug resistance, a combination of alterations in the CYP51 was required for effective azole resistance.

Several paralogs of the CYP51 were usually found in various fungal genomes named as CYP51A, B and C, with CYP51C being reported exclusively from *Fusarium* (Fan *et al.* 2013). Fungi with multiple CYP51s have inherent resistance to azoles, although some azole fungicides still effective against almost all pathogenic fungus. For instance, although fluconazole is ineffective, voriconazole and itraconazole control *A. fumigatus* very well. Resistance to azole drugs in fungi with multiple CYP51s is mainly mediated by the change of CYP51B (Gao *et al.* 2018). Thus,

To cite this paper: Liao W, T Liu, W Liao, J Yang (202x). Substrate recognition site 5 of CYP51 protein contributes to azole binding in rice blast fungus *Maganporthe oryzae*. *Intl J Agric Biol* 00:000–000

CYP51B could be stated as an important target region in *M. oryzae* for antifungal drug development.

In this study, we investigated the roles of several key conserved residues of SRS5 and SRS6 domains of the of CYP51 protein from *M. oryzae* (MoCYP51B) in binding to diniconazole. Through site directed mutagenesis and binding spectra analysis, we revealed the important roles of I367 and V374 in azole sensitivity. Both the residues conserved amino acids in the SRS5 region of MoCYP51B. This study provides additional evidence in support of the role of SRS5 region of CYP51B protein in azole binding in addition to broadening our knowledge about the various amino acid residues contributing to this interaction. This information will probably take us a step further in designing effective and specific inhibitors against pathogenic attack.

Materials and Methods

Strains

Wild-type *M. oryzae* was obtained from the Agricultural Culture Collection of China (ACCC preservation number 30320), Beijing, China. Fungal spores were preserved in sterile water storage at room temperature. *Escherichia coli* BL21 (DE3) were purchased from Novagen (Germany). Bacterial cultures were maintained in glycerol stocks at -80°C. Working stocks were maintained as liquid cultures at 4°C.

Cloning of the *MoCYP51B* gene and construction of expression vector

Genomic DNA was extracted using the E.Z.N.A. DNA kit (Omega, USA), and the DNA concentration was measured at OD_{260} by NanoDrop™ 2000 spectrophotometer (Thermo Fisher Scientific, U.S.A.). The truncate *MoCYP51B* was amplified using primers F (5'-GATATCCGTCCCAAATCGGAACCA-3') and R (5'-CCGCTCGAGTTGTCATTCTACGCAGTCTTCG-3'), with inserted EcoRV and XhoI restriction sites, respectively. The DNA fragment ligated to pET30a (+) vector (Novagen, Germany). The success of the cloning was cross-checked with enzyme digestion of the plasmid followed by sequencing.

Sequence alignment and analysis of CYP51s

The nucleotide and amino acid sequences were obtained from the cytochrome P450 homepage and NCBI Data Bank. In order to compare the inter specific amino acid sequences of CYP51s, the nucleotide sequences of *cyp51* exons across species were translated into their corresponding amino acids using the software EMBOSS: transeq (http://www.ebi.ac.uk/emboss/transeq/). The sequences were aligned, using the clustalW 1.82 program (http://www.ebi.ac.uk/clustalw/).

Site-directed mutagenesis

Several key conserved amino acids in SRS5 and SRS6 domains of CYP51 family were selected for site-directed mutagenesis. Desired mutations were introduced into pET30a (+)-*MoCYP51B* using a site-directed mutagenesis kit (SBS Genetech Co., Ltd., China), using 200 ng of (pET30a(+)-*MoCYP51B)* plasmid and 10 μM of each primer (Table 1).

Expression and extraction of recombinant proteins

The constructed plasmid pET30a (+)-*Mo*CYP51B was transformed into *E. coli* BL21(DE3). The cells were cultivated at 37°C and 210 rpm in LB medium and OD_{600} was checked to determine the growth phase of the culture every 2 h. After the cultures reached the desired OD_{600} of 0.5–0.6, 0.5 m*M* IPTG was added. Cells were harvested after 2 h, and the bacterial pellet obtained from 1 L of initial culture was suspended in 50 mL 25 m*M* Tris-HCl (pH 7.5) and kept at -70°C. Frozen cells were sonicated in Tris-HCl containing 2 m*M* DTT using an Ultrasonic Probe 2000 Sonicator (Trading, China) at 30% power for 10 min (10 s sonication, 10 s rest), and centrifuged at 4°C to remove cell debris. The membrane fractions were suspended in 100 m*M* potassium phosphate (pH 7.5) buffer containing 20% glycerol, 1 m*M* reduced glutathione, and 0.1 m*M* EDTA. The protein content was measured using a bicinchoninic acid protein assay kit (Sigma-Aldrich, USA) with BSA as a standard.

Western blot analysis

To detect the wild-type and mutant MoCYP51 proteins, the cell extracts were fractionated by SDS-PAGE using 12% gels and transferred to a nitrocellulose membrane electrophoretically (Novagen, USA). The membrane was then probed with mouse anti-His CYP51 IgG, conjugated with anti-mouse IgG (H + L) (Pierce, USA).

Reduced CO-difference spectrum

The CYP450 protein content and activity were tested as reported previously (Omura and Sato 1964). In order to record the baseline, microsomal suspensions were reduced with by using a few milligrams of solid sodium dithionite and transferred to quartz cuvettes. A S3100 UV-visible spectrophotometer (Twin Lakers, USA) was used for all recording. The contents of the sample cuvettes were subsequently bubbled with CO for a pulse of 50 s (1 bubble s^{-1}) with simultaneous recording of the spectral differences. Microsomal P450 (250 pmol) with 5 m*M* azole fungicide (0.9% DMSO used as control) was kept on ice briefly (3–5 min). The CO difference spectrum (reduced) was recorded at a stretch of 50 min with 10 min intervals at the onset of CO treatment.

Diniconazole binding spectra

Diniconazole was purchased from the Factory of Limin (Yancheng, China). Diniconazole binding spectra were detected by using S3100 UV-visible scanning spectrophotometer (Sinco, Korea). The baseline was recorded for 250 pmol microsomal suspensions. Differences in spectra were noted by addition of increasing concentration of diniconazole (dissolved in DMSO). The data points are fitted to a rectangular hyperbola, and the K_d value was generated by the equation $\Delta A = \Delta A_{max} [I]/(K_d + [I])$. The binding experiments were repeated three times and the results were interpreted based on triplicate observations.

Results

Multiple sequence alignment of CYP51 proteins in fungi

To identify the essential residues for maintaining protein structure and function, members of CYP51 family from various fungal species were aligned (Fig. 1). In the SRS5 region, the residues I367, R372 and V374 showed an absolute conservation nearly in all the species. In the SRS6 region, complete conservation is observed for S494 and P499. All these residues are marked with the triangle symbol (Fig. 1). In order to assess the function of conserved amino acids in MoCYP51B active cavity, amino acid subsets I367, R372, V374 in the SRS5 and S494, P499 in the SRS6 were selected for site-directed mutagenesis.

Expression and detection of wild-type and mutant MoCYP51B proteins

Based on the results of sequence alignment, the absolute conservation residues were selected for further analysis. Using site-directed mutagenesis methods, we mutated I367, R372, V374 and S494, P499 in the SRS5 and SRS6 regions, respectively, followed by the bacterial expression of protein. The motilities of the MoCYP51B proteins upon expression were coincident with their theoretical molecular weights (approximately 51 kD). The detection of the band of the protein of interest was performed by Western blotting (Fig. 2). All the recombinant proteins produced a CO reduced difference spectrum with Soret peak around 447 nm. Thus, the results suggested a conservation of the functionalities of the proteins even after introduction of point mutations.

Diniconazole binding to mutated MoCYP51B protein

The azole fungicide, diniconazole, forms a type-II binding spectra upon binding to active cavity of the purified MoCYP51B protein. A similar spectrum with maximum absorbance at 428 nm and a minimum at 395 nm has been observed after diniconazole binding with *Penicillium digitatum* CYP51 protein (Zhao *et al.* 2007). No alteration in the structure and function of the various mutated

Table 1: Primers used for site-directed mutagenesis

Primer	Sequence (5′-3′)	Introduced CYP51 mutant
Mo-I367Lmut	CGGGTGCACTCGTCCCTCCACTCCATCATGC	I367L
Mo-I367Wmut	GGGTGCACTCGTCCTGGCACTCCATCATGCG	I367W
Mo-R372Dmut	ATCCACTCCATCATGGACAAGGTGAAGCGGCC	R372D
Mo-V374Amut	CCATCATGCGCAAGGCGAAGCGGCCGATGC	V374A
Mo-V374Ymut	CCATCATGCGCAAGTACAAGCGGCCGATGCG	V374Y
Mo-S494Fmut	CCCACTGATTACACTTTTATGTTCTCTCGGCCT	S494F
Mo-S494Tmut	CCCACTGATTACACTACTATGTTCTCTCGGC	S494T
Mo-P499Emut	TCTATGTTCTCTCGGGAGATGCAGCCTGCGACG	P499E
Mo-P499Qmut	TCTATGTTCTCTCGGCAGATGCAGCCTGCGACG	P499Q

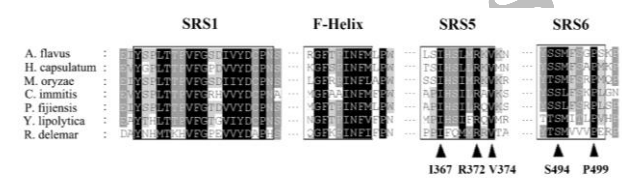

Fig. 1: Multiple alignment of CYP51Bs. The sequences of DNA and deduced amino acids were aligned using the computer program clustalw 1.82 (http://www.ebi.ac. uk/clustalw/). The conserved residues in MoCYP51 active cavity for SRS5 and SRS6 are marked with the triangle symbol

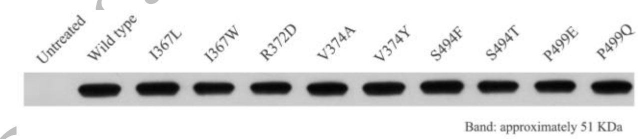

Fig. 2: Western blotting for heterologous expression of recombinant MoCYP51 proteins. The filter was probed with mouse anti-His CYP51 IgG, conjugated with antimouse IgG (H + L). Untreated: IPTG uninduced

MoCYP51B proteins was observed. All the wild type and mutated proteins bound to diniconazole formed a type-II binding spectra with with peak located at 410–415 nm and a trough at 375–380 nm. The mutated MoCYP51B proteins could bind to diniconazole, although K_d values varied (Fig. 3). Compared to the wild type protein, the K_d values of the mutations I367L, R372D, V374A, S494F, S494T, P499E and P499Q upon binding to diniconazole were essentially unchanged, whereas the K_d value of V374Y and I367W increased significantly ($P < 0.05$) (Table 2), indicating that the binding efficiency of these two mutated proteins significantly decreased. Based on previous results and current spectral analysis, an interaction between triazoles and the heme of CYP450 lead to the mode transition to high-spin state can be suggested. In turn, this would cause the sixth ligand of heme iron to be replaced by the nitrogen atom in the triazole ring of diniconazole (Buckner *et al.* 2003).

Discussion

The increased resistance of fungi to azole antibiotics could be due to excessive use of azole fungicides. However, the complex mechanism of drug resistance in fungal is still not

Table 2: The K_d value of recombinant protein bound to diniconazole

Recombinant protein	Regressive equation	$K_d \pm SD(\mu M)$
Wild-type	y = 2.4439x - 0.0493	0.017 ± 0.004
I367L	y = 1.0457x + 0.1143	0.042 ± 0.007
I367W	y = 1.1572x + 0.0413	0.130 ± 0.064
R372D	y = 2.0928x + 0.059	0.030 ± 0.002
V374A	y = 0.8165x + 0.0186	0.063 ± 0.024
V374Y	y = 0.4748x + 0.0882	0.178 ± 0.012
S494F	y = 0.9123x + 0.0822	0.056 ± 0.034
S494T	y = 1.0098x + 0.0648	0.085 ± 0.030
P499E	y = 1.0981x + 0.0641	0.053 ± 0.007
P499Q	y = 1.191x + 0.1154	0.069 ± 0.040

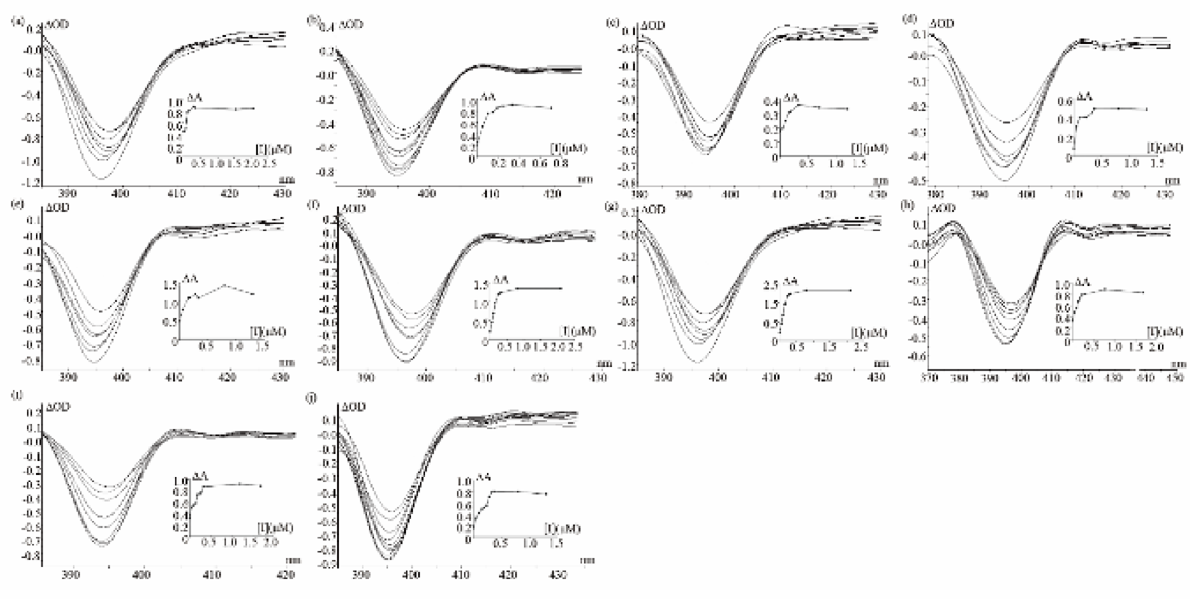

Fig. 3: Binding spectra in the presence of diniconazole for the wild type and mutant SRS5 and SRS6 of MoCYP51 (protein content 1 g/L). (**a**): the wild-type CYP51 protein; (**b**): CYP51 with I367L mutation; (**c**): CYP51 with I367W mutation; (**d**): CYP51 with R372D mutation; (**e**): CYP51 with V374A mutation; (**f**): CYP51 with V374Y mutation; (**g**): CYP51 with S494F mutation; (**h**): CYP51 with S494T mutation; (**i**): CYP51 with P499E mutation; (**j**): CYP51 with P499Q mutation. The main section of the figure shows difference spectra induced by diniconazole binding to wild type and mutated MoCYP51B proteins. The inset shows the relation between diniconazole concentrations and the magnitude of type-II difference spectra (A410-415 minus A375-380). The data points are fitted to a rectangular hyperbola, and the K_d value was generated by the equation $\Delta A = \Delta A_{max}[I]/(K_d + [I])$

very clear (Fan *et al.* 2013). To date, several amino acid residues associated with fungicide sensitivity in fungal protein CYP51B have been identified. More than 140 different point mutations in the *Candida albicans* CYP51B have been found to lower the binding affinity of the protein to the fungicide. Of specific interest is the mutataion S279F/Y that had a 4- to 5-folds lower affinity for fluconazole and 3.5-fold lower affinity for voriconazole in comparison to the wild-type protein (Warrilow *et al.* 2012). Azole binding mechanism to CYP51 protein has been thoroughly studied in *Mycosphaerella graminicola.* Cools *et al.* (2011) suggested that the substitution S524T of MgCYP51 variants lead to the decreased efficacy of epoxiconazole and prothioconazole. Our previous research identified the presence of a hydrophobic site P222 in F helix of MoCYP51, which could play a very important role in modulating the affinity for azole fungicides (Liao *et al.* 2015). In this study, several important conserved amino acids in these two domains of MoCYP51B were mutated followed by thorough binding analysis *via* spectophotometry. The results showed that the conserved residues I367 and V374 in SRS5 contribute to diniconazole binding and mutations I367W and V374Y significantly reduced the binding affinity.

According to the molecular modeling study of azole agents with *C. albicans* CYP51, it was found that residues L376 and S378, either of which is not conserved in SRS5 of CYP51s family, might play an important role in binding of the inhibitor or substrate (Chen *et al.* 2009). It is worth to note that the substitution of nonpolar hydrophobic residue

I367 with the nonpolar aromatic W, concomitantly reduces the binding ability of MoCYP51 to diniconazole, while a substitution to the nonpolar hydrophobic residue L has no effect, indicating that the aromatic side chain probably hinders the affinity towards the azole fungicide. In addition, the substitution of nonpolar hydrophobic residue V374 by the polar Y reduces the binding ability of MoCYP51 to diniconazole, whereas the substitution by nonpolar A had no effect, indicating that the hydrophobicity of this site may be important for the affinity towards the azole fungicide. According to previous molecular modeling study of azole agents with *C. albicans* CYP51 (Chen *et al.* 2009), it was found that residues I367 and S378 in the SRS5 region of CYP51 protein played an important role in inhibitor binding to the substrate.

Strushkevich *et al.* (2010) suggested that, in human SRS6 region of CYP51B, the main-chain carbonyl group of M487-corresponding residue forms a hydrogen bond with the 3β-hydroxy group of substrate analog aiding substrate recognition. Contrary to these findings, our results indicate that in *M. oryze*, conserved residues of the SRS6 domain of MoCYP51B do not contribute to substrate sensitivity. Specifically, point mutations resulting in the substitutions S494T/F and P499E/Q in SRS6 domain of MoCYP51B have no effect on the binding intensity of the protein to azoles. Recent outbreaks of resistant strains of MoCYP51 variants have limited the affectivity of the most potent azole fungicides. Until and unless this evolution of the newer variants is kept on check, the azole drugs will be of little help in near future. An extensive genetic analysis needs to be carried out to elucidate the mechanisms of azole-fungi interactions. As the azole drugs have been in use for a long time, a potential formulation of azole drug combination can only be suggested as a remedy to arrest the constantly changing molecular machinery of *M. oryzae* to combat the fungicides.

More understanding of structure/function relations for key amino acid residues of CYP51 protein will open an opportunity for design of novel highly effective fungicides. In this paper, we investigated the azole binding potency of conserved residues of SRS5 and SRS6 regions in MoCYP51B protein. The data revealed the residues I367 and V374 in MoCYP51B SRS5 had critical contribution to azole binding. This information will help for the development of novel antifungal agents against *M. oryzae*.

Conclusion

The amino acid residues I367 and V374 in the MoCYP51B SRS5 played an important role in the azole binding. Further studies are needed to the design of effective and specific DMIs for *M. oryzae*.

Acknowledgements

This research was supported by the Hubei Provincial Natural Science Foundation of China (No. 2019CFB265), and the Research and Innovation Initiatives of WHPU (No. 2019Y03).

Author Contributions

Conceived and designed the experiments: WFL and JYY. Performed the experiments: TTL and WFL. Analyzed the data: TTL and WJL. Contributed reagents/materials/analysis tools: JYY. Wrote the paper: WFL.

References

Buckner FS, K Yokoyama, JW Lockman, K Aikenhead, J Ohkanda, M Sadilek, MH Gelb (2003). A class of sterol 14-demethylase inhibitors as anti-*Trypanosoma cruzi* agents. *Proc Natl Acad Sci USA* 100:15149–15153

Chen SH, CQ Sheng, XH Xu, YY Jiang, WN Zhang, C He (2009). Expression and detection the enzyme activity of the wild and mutation type of CYP51 protein of *Candida albicans*. *Microbiol Bull* 10:1564–1570

Chen XL, YL Jia, BM Wu (2019). Evaluation of rice responses to the blast fungus *Magnaporthe oryzae* at different growth stages. *Plant Dis* 103:132–136

Chowdhary A, S Kathuria, HS Randhawa, SN Gaur, CHW Klaassen, JF Meis (2012). Isolation of multiple-triazole-resistant *Aspergillus fumigatus* strains carrying the TR/L98H mutations in the cyp51A gene in India. *J Antimicrob Chemother* 67:362–366

Cools HJ, JGL Mullins, BA Fraaije, JE Parker, DE Kelly, JA Lucas, SL Kelly (2011). Impact of recently emerged sterol 14 alpha-demethylase (CYP51) variants of *Mycosphaerella graminicola* on azole fungicide sensitivity. *Appl Environ Microbiol* 77:3830–3837

Fan J, M Urban, JE Parker, HC Brewer, SL Kelly, KE Hammondkosack, HJ Cools (2013). Characterization of the sterol 14 alpha-demethylases of *Fusarium graminearum* identifies a novel genus-specific CYP51 function. *New Phytol* 198:821–835

Gao P, YL Cui, RL Wu (2018). Molecular dynamic modeling of CYP51B in complex with azole inhibitors. *J Biomol Struct Dyn* 36:1511–1519

Hargrove TY, Z Wawrzak, DC Lamb, FP Guengerich, GI Lepesheva (2015). Structure-functional characterization of cytochrome P450 sterol 14 alpha-demethylase (CYP51B) from *Aspergillus fumigatus* and molecular basis for the development of antifungal drugs. *J Biol Chem* 290:23916–23934

Hargrove TY, Z Wawrzak, J Liu, WD Nes, MR Waterman, GI Lepesheva (2011). Substrate preferences and catalytic parameters determined by structural characteristics of sterol 14 alpha-demethylase (CYP51) from *Leishmania infantum*. *J Biol Chem* 286:26838–26848

Jeon JB, G Lee, K Kim, S Park, S Kim, S Kwon, A Huh, H Chung, D Lee, CW Kim, Y Lee (2020). Transcriptome profiling of the rice blast fungus *Magnaporthe oryzae* and its host *Oryza sativa* during infection. *Mol Plant Microb Interact* 33:141–144

Lamb DC, DE Kelly, NJ Manning, DW Hollomon, SL Kelly (1998). Expression, purification, reconstitution and inhibition of *Ustilago maydis* sterol 14 alpha-demethylase (CYP51; P450(14DM)). *FEMS Microbiol Lett* 169:369–373

Lepesheva GI, MR Waterman (2007). Sterol 14 alpha-demethylase cytochrome P450 (CYP51), a P450 in all biological kingdoms. *Biochim Biophys Acta* 1770:467–477

Liao WF, TT Liu, S Yang, GS Zhang, T Shu, JY Yang (2015). Interaction between the conserved amino acid in *Magnaporthe oryzae* CYP51F helix and Diniconazole. *Microbiol Bull* 42:2433–2439

Liu H, WX Tian, B Li, GX Wu, M Ibrahim, ZY Tao, GL Xie (2012). Antifungal effect and mechanism of chitosan against the rice sheath blight pathogen, *Rhizoctonia solani*. *Biotechnol Lett* 34:2291–2298

Lopez AL, CJ Cumagun (2019). Genetic structure of *Magnaporthe oryzae* populations in three island groups in the Philippines. *Eur J Plant Pathol* 153:101–118

Omura T, R Sato (1964). The carbon monoxide-binding pigment of liver microsomes. I. Evidence for its hemoprotein nature. *J Biol Chem* 239:2370–2378

Parker JE, AGS Warrilow, HJ Cools, CM Martel, WD Nes, BA Fraaije, SL Kelly (2011). Mechanism of binding of prothioconazole to *Mycosphaerella graminicola* CYP51 differs from that of other azole antifungals. *Appl Environ Microb* 77:1460–1465

Price CL, AGS Warrilow, JE Parker, JGL Mullins, WD Nes, DE Kelly, SL Kelly (2015). Novel substrate specificity and temperature-sensitive activity of *Mycosphaerella graminicola* CYP51 supported by the native NADPH Cytochrome P450 reductase. *Appl Environ Microbiol* 81:3379–3386

Strushkevich N, SA Usanov, HW Park (2010). Structural basis of human cyp51 inhibition by antifungal azoles. *J Mol Biol* 397:1067–1078

Talbot NJ (2003). On the trail of a cereal killer: Exploring the biology of *Magnaporthe grisea. Annu Rev Microbiol* 57:177–202

Warrilow AGS, JGL Mullins, CM Hull, JE Parker, DC Lamb, DE Kelly, SL Kelly (2012). S279 point mutations in *candida albicans* Sterol 14-alpha Demethylase (CYP51) reduce *in vitro* inhibition by fluconazole. *Antimicrob Agents Chemother* 56:2099–2107

Yan L, Q Yang, Y Zhou, X Duan, Z Ma (2013). A real-time PCR assay for quantification of the Y136F allele in the CYP51 gene associated with *Blumeria graminis* f. spp. *tritici* resistance to sterol demethylase inhibitors. *Crop Prot* 28:376–380

Yang JY, Q Zhang, MJ Liao, M Xiao, WJ Xiao, S Yang, J Wan (2009). Expression and homology modelling of sterol 14 alpha-demethylase of *Magnaporthe grisea* and its interaction with azoles. *Pest Manage Sci* 65:260–265

Zhao L, D Liu, Q Zhang, S Zhang, J Wan, W Xiao (2007). Expression and homology modeling of sterol 14 alpha-demethylase from *Penicillium digitatum. FEMS Microb Lett* 277:37–43